doi:10.1093/jmcb/mjy038
Published online July 16, 2018

Article

Interleukin-6 secretion is limited by self-signaling in endosomes

Daniëlle R. J. Verboogen[1], Natalia H. Revelo[1], Martin ter Beest[1], and Geert van den Bogaart[1,2,*]

[1] Department of Tumor Immunology, Radboud Institute for Molecular Life Sciences, Radboud University Medical Center, 6525 GA Nijmegen, The Netherlands
[2] Department of Molecular Immunology, Groningen Biomolecular Sciences and Biotechnology Institute, University of Groningen, Nijenborgh 7, 9747 AG Groningen, The Netherlands
* Correspondence to: Geert van den Bogaart, E-mail: g.van.den.bogaart@rug.nl

Edited by Bing Su

Cells producing cytokines often express the receptor for the same cytokine, which makes them prone to autocrine signaling. How cytokine release and signaling are regulated in the same cell is not understood. In this study, we demonstrate that signaling by exogenous and self-synthesized inflammatory cytokine interleukin-6 (IL-6) within endosomal compartments acts as a cellular brake that limits the synthesis of IL-6. Our data show that IL-6 is internalized by dendritic cells and signals from endosomal compartments containing the IL-6 receptor. Newly synthesized IL-6 also traffics via these endosomal compartments and signals in transit to the plasma membrane. This allows activation of STAT3 which in turn limits toll-like receptor 4 stimulant lipopolysaccharide (LPS) triggered transcription of IL-6. Long-term exposure to LPS removes this brake via inhibition of STAT3 by increased expression of suppressor of cytokine signaling 3 and results in fully fledged IL-6 production. This transient regulation could prevent excessive IL-6 production during early infections.

Keywords: membrane trafficking, cytokine release, exocytosis, interleukin-6, endosomal signaling

Introduction

Interleukin-6 (IL-6) is the most pleiotropic cytokine known in mammals (Ernst and Jenkins, 2004). It has both pro- and anti-inflammatory properties and is involved in the pathogenesis of all inflammatory diseases (Wolf et al., 2014; Garbers et al., 2015; Tanaka et al., 2016). IL-6 can promote the activation, growth, proliferation, and survival of many different cell types (Hunter and Jones, 2015). IL-6 production by immune phagocytes is triggered by a wide range of stimuli, such as stress hormones, cytokines, and pathogen recognition by toll-like receptors (TLRs) (Dittrich et al., 1994). In healthy individuals, blood levels of free IL-6 (i.e. not in complex with soluble IL-6 receptor) are in the low pg/ml range, depending on the assays used because not every assay can distinguish between free and complexed IL-6 (Helfgott et al., 1989; May et al., 1992, 1994; Ndubuisi et al., 1998). In contrast, blood levels of IL-6 can increase to ng/ml range in autoimmune diseases and to μg/ml range during septic shock (Grossman et al., 1989; Waage et al., 1989; Damas et al., 1992; Robak et al., 1998; Nowell et al., 2003; Chaudhry et al., 2013; Shimamoto et al., 2013). In addition, IL-6 levels correlate with tumor progression in many cancer types (Salgado et al., 2003; Yu et al., 2007; Xu et al., 2016). IL-6 induces the development of Th17 cells while inhibiting differentiation of regulatory T cells. These T cell subsets have key functions in immune regulation: IL-17-producing Th17 cells protect against microbial infections but also contribute to the pathogenesis of many autoimmune diseases, including multiple sclerosis and rheumatoid arthritis, whereas regulatory T cells limit excessive effector T cell responses (Kimura and Kishimoto, 2010). Differentiation of pathogenic Th17 cells mainly occurs by presentation of IL-6 loaded onto the IL-6 receptor on the surface of dendritic cells, in a process called *trans*-presentation (Heink et al., 2017).

The IL-6 receptor consists of IL-6 receptor alpha (IL-6RA, CD126, gp80) and the signal transducing subunit glycoprotein 130 (gp130, CD130) (Schaper and Rose-John, 2015). IL-6 first binds to IL-6RA with a low affinity dissociation constant of ~10 nM (Yamasaki et al., 1988; Dittrich et al., 1994). This complex of IL-6 with IL-6RA in turn binds to two molecules of gp130 with two orders of magnitude higher affinity, resulting in a net

Received December 4, 2017. Revised May 4, 2018. Accepted July 12, 2018.

dissociation constant in the pM to nM range (Zohlnhöfer et al., 1992; Dittrich et al., 1994; Hammacher et al., 1994). Following oligomerization, Janus tyrosine kinases (JAK) phosphorylate the intracellular tails of gp130 which in turn recruit and activate signal transducer and activator of transcription (STAT) and mitogen-activated protein kinase (MAPK) signaling systems (Ernst and Jenkins, 2004; Silver and Hunter, 2010). In addition to the activation of STAT3 by phosphorylation of tyrosine 705, its activity is further promoted by phosphorylation at serine 727 (Wen et al., 1995; Galdiero et al., 2006; Moravcová et al., 2016) by the mammalian target of rapamycin (mTOR) (Yokogami et al., 2000) or protein kinase C delta (PKCδ) (Bhattacharjee et al., 2006). In contrast to IL-6RA, which is specific for IL-6, gp130 is shared by all cytokines of the IL-6 family: IL-11, leukemia inhibitory factor (LIF), oncostatin M (OsM), cardiotrophin-1 (CT-1), ciliary neurotrophic factor (CNTF), and cardiotrophin-like cytokine (CLC) (Ernst and Jenkins, 2004). Whereas gp130 is ubiquitously expressed in hematopoietic and non-hematopoietic cells, IL-6RA is expressed only by a limited number of cell types, such as hepatocytes and immune cells (Larregina et al., 1997; McFarland-Mancini et al., 2010; Silver and Hunter, 2010; Wolf et al., 2014; Garbers et al., 2015).

Interestingly, many leukocytes (monocytes, dendritic cells, macrophages, B cells) that produce IL-6 also express IL-6RA (Hwang et al., 2010), enabling autocrine signaling. Although IL-6 was originally believed to promote activation and maturation of dendritic cells (Jonuleit et al., 1997), it is increasingly clear that IL-6 inhibits these processes via STAT3 activation (Park et al., 2004; Yu et al., 2007; Melillo et al., 2010). In line with this previously described inhibitory role, IL-6 knockout mice show enhanced activation compared to wild-type (Wang et al., 2004; Melillo et al., 2010). IL-6 also influences activation of other immune cells as it, for instance, blocks the proliferation of proinflammatory M1 macrophages in mice (Luig et al., 2015). STAT3 activation interferes with TLR signaling, as pre-treatment of dendritic cells with IL-6 reduces maturation triggered by lipopolysaccharide (LPS), a bacterial TLR4 stimulus, and leads to decreased expression of the maturation markers CD86 and MHC class II (Park et al., 2004). LPS in turn is well known to inhibit tyrosine phosphorylation of STAT3 (pY-STAT3) (Meley et al., 2017) and promote IL-6 synthesis by dendritic cells (van Bon et al., 2010; Kumolosasi et al., 2014), raising the question of how this cross-talk between STAT3 and TLR4 signaling would affect cellular responses to IL-6 and LPS.

In this study, we investigated how signaling of self-synthesized IL-6 affects the production of IL-6 by dendritic cells. By microscopy, we show that newly synthesized IL-6 traffics from the Golgi network to the plasma membrane via recycling endosomes, a network of tubulovesicular compartments that interconnects endocytic and exocytic trafficking pathways, as previously shown for macrophages (Manderson et al., 2007) and dendritic cells (Verboogen et al., 2018). We hypothesized that newly synthesized IL-6 in transit to the plasma membrane could signal from these recycling endosomal compartments, since IL-6 has been described to signal from endosomes in hepatocytes (Shah et al., 2006; Xu et al., 2007; German et al., 2011). Indeed, we found that in dendritic cells pY-STAT3 signaling is initiated by binding of both internalized IL-6 and newly synthesized IL-6 to IL-6RA within intracellular compartments. This signaling results in a negative feedback loop and acts as a brake limiting IL-6 synthesis. However, long-term exposure to LPS releases this brake, as pY-STAT3 is inhibited by a LPS-induced increase of expression of suppressor of cytokine signaling 3 (SOCS3), a previously described suppressor of STAT3 signaling (Croker et al., 2003, 2012; Lang et al., 2003), and this allows full IL-6 production. Thus, our data show that self-signaling by newly synthesized IL-6 limits the production of IL-6 during short-term exposure to the inflammatory stimulus LPS. This mechanism might serve to restrain IL-6 responses during early infection and sepsis.

Results

Cross-inhibition of IL-6 and LPS signaling in dendritic cells

We first confirmed that the IL-6 receptor is expressed by dendritic cells. Reverse transcription (RT)-PCR, western blot, and flow cytometry showed that IL-6RA is expressed by human $CD1c^+$ myeloid and $BDCA4^+$ plasmacytoid dendritic cells (mDC and pDC) isolated from the blood of healthy donors (Figure 1A and Supplementary Figure S1A–E). IL-6RA is also expressed by dendritic cells differentiated from human blood-isolated monocytes (moDCs) by granulocyte macrophage colony-stimulating factor (GM-CSF) and IL-4, as reported previously (Meley et al., 2017). Moreover, mouse bone marrow-derived dendritic cells (BMDCs) differentiated by either GM-CSF or fms-related tyrosine kinase 3 ligand (FLT3L) expressed IL-6RA, as reported previously (Hwang et al., 2010), as well as the murine macrophage cell line RAW264.7. IL-6RA can be expressed as a long transmembrane isoform and as a short soluble isoform lacking its transmembrane helix and cytoplasmic domain (Wolf et al., 2014; Garbers et al., 2015). Soluble IL-6RA can also be produced by shedding of the long isoform of IL-6RA from the cell membrane (Müllberg et al., 1993, 1994) by metalloproteases ADAM10 and ADAM17 (Matthews et al., 2003; Yan et al., 2016; Zunke and Rose-John, 2017). For western blot, we used an antibody recognizing the cytoplasmic C-terminal tail of IL-6RA, meaning that only the full-length membrane bound form of IL-6RA was detected. However, transcription of the short isoform was also detected by RT-PCR with isoform-specific primers (Horiuchi et al., 1994) (Supplementary Figure S1C). Moreover, the short soluble isoform of IL-6RA was detected in the supernatant of moDCs by ELISA, as recently shown (Meley et al., 2017), and this was independent of the presence of LPS (Supplementary Figure S1F).

Although the expression levels of IL-6RA varied widely among donors/mice, repeats and conditions, western blot experiments showed that IL-6RA expression did not change significantly after stimulation with LPS up to 24 h in GM-CSF and FLT3L-differentiated BMDCs and RAW264.7 macrophages (Figure 1A and Supplementary Figure S1A). Similarly, western blot and flow cytometry experiments revealed that IL-6RA expression did not change significantly in primary mDCs after overnight stimulation with LPS or with a

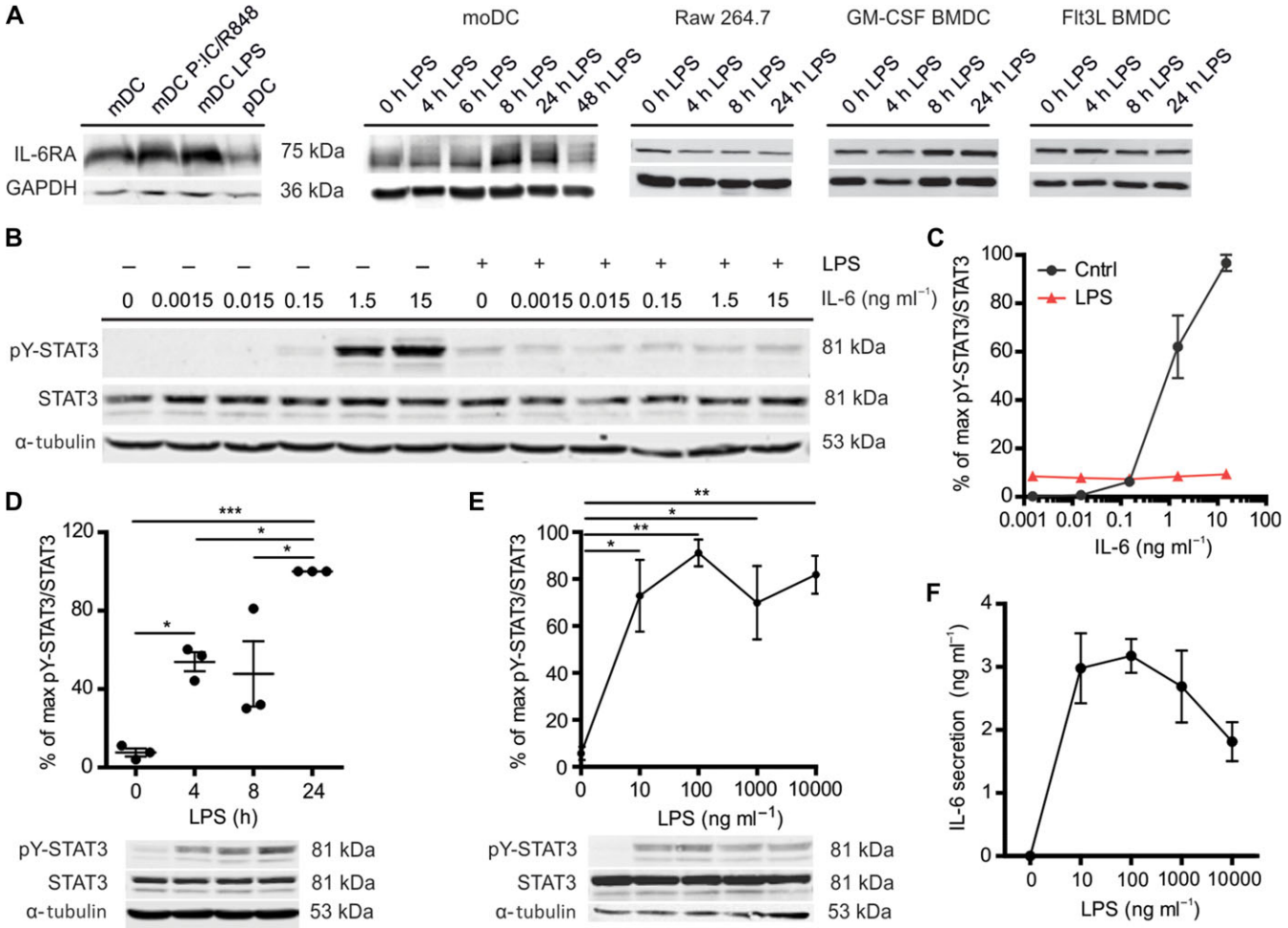

Figure 1 LPS induces STAT3 tyrosine phosphorylation but inhibits IL-6-mediated STAT3 tyrosine phosphorylation in dendritic cells. (**A**) IL-6RA expression by western blot for mDC with or without overnight stimulation with LPS or a combination of Poly(I:C) and R848, for pDC, and for moDCs, RAW264.7, and murine GM-CSF, and FLT3L-differentiated BMDCs stimulated with LPS for the indicated times. GAPDH is loading control. Quantification for multiple donors is shown in Supplementary Figure S1A. (**B**) STAT3 tyrosine 705 phosphorylation (pY-STAT3) by western blot. MoDCs were incubated with the indicated IL-6 concentrations for 20 min with or without 4 h LPS pre-incubation. α-tubulin is loading control. Results from the other three donors are shown in Supplementary Figure S2A. (**C**) Quantification of pY-STAT3/STAT3 in **B** (error bars represent SEM for four donors; see Supplementary Figure S2A). Data were normalized to the highest ratio of pY-STAT3 over STAT3 per donor. (**D**) pY-STAT3 by western blot. moDCs were incubated with LPS for 4, 8, or 24 h (data from individual donors are shown). (**E**) pY-STAT3 of moDCs incubated with the indicated LPS concentrations for 4 h by western blot. (**F**) IL-6 concentration in the medium collected from the cells in **E** by ELISA.

combination of the TLR3 agonist polyinosinic:polycytidylic acid (poly(I:C)) and the TLR7/8 agonist R848, nor in plasmacytoid dendritic cells stimulated with the TLR9 agonist CpG-C (Figure 1A; Supplementary Figure S1A and D).

For the rest of the experiments, we focused on moDCs, a widely used model system for immune cell function capable of producing large amounts of IL-6 (van Bon et al., 2010; Verboogen et al., 2018). MoDCs do not only express IL-6RA but also the signaling co-receptor gp130 (Figure 1A; Supplementary Figure S1A, E–G). The soluble form of gp130, which is produced by shedding of full-length gp130 from the cell membrane, could also be detected in the supernatant by ELISA after 24 h incubation with LPS (Supplementary Figure S1H). For some donors, LPS resulted in lower levels of IL-6RA and gp130, but this was not consistent as no changes were observed for other donors, and, although there was a trend towards overall lower IL-6RA and gp130 levels, the donor-averaged cellular levels of gp130 and IL-6RA did not significantly change upon LPS stimulation (Figure 1A; Supplementary Figure S1A, D–H). In line with this, comparison of the profiles of the IL-6RA bands of the western blots suggested that the glycosylation states of IL-6RA did not significantly change upon LPS treatment (Supplementary Figure S1I). These results contrast the observations by Meley et al. (2017) that short-term (up to 8 h) LPS treatment resulted in a slight decrease of IL-6RA levels whereas longer incubations result in higher levels of IL-6RA, and gp130 levels decreased

strongly upon LPS treatment, possibly because of the large donor variation or the source of LPS used. IL-6RA and gp130 are capable of forming a signaling-competent complex, as culturing in the presence of IL-6 concentrations above 0.15 ng/ml resulted in tyrosine phosphorylation of STAT3 (pY-STAT3, Tyr705) in a concentration-dependent manner (Figure 1B and C; Supplementary Figure S2A and B). In contrast, serine phosphorylation of STAT3 (pS-STAT3, Ser727) was already observed in the absence of IL-6 and only increased at the highest concentration of IL-6 tested (15 ng/ml; Supplementary Figure S2B).

Next, we tested whether LPS stimulation of the moDCs would block STAT3 activation, as has been described (Niemand et al., 2003; Bode et al., 2012; Meley et al., 2017). Indeed, LPS partially blocked STAT3 activation, as levels of pY-STAT3 by IL-6 were reduced when we pre-cultured the cells for 4 h with LPS prior to the addition of IL-6 (~90% reduction for 15 ng/ml IL-6 compared to without LPS) (Figure 1B and C; Supplementary Figure S2A and B). In contrast, LPS did not affect serine phosphorylation for all concentrations of IL-6 tested, except for the highest concentration of 15 ng/ml IL-6, where we observed a slight reduction of serine phosphorylation (Supplementary Figure S2B). Tyrosine phosphorylation of STAT3 in the presence of LPS was no longer dependent on the concentration of IL-6, but already 10 ng/ml LPS (i.e. the lowest concentration of LPS tested) without IL-6 resulted in tyrosine phosphorylation of STAT3 in a time-dependent fashion, albeit with slower kinetics than IL-6-mediated pY-STAT3 phosphorylation (Figure 1D and E), and as previously shown (Meley et al., 2017). This increase was likely caused by autocrine signaling, as LPS promoted transcription of IL-6 (Supplementary Figure S2C) resulting in IL-6 production to a final concentration of approximately 3 ng/ml (Figure 1F). These results demonstrate that already low concentrations of LPS partially, but not completely, block activation of pY-STAT3 by IL-6. In order to further investigate the molecular basis for this LPS block of pY-STAT3 signaling, we looked into SOCS3 activation, a well-known negative regulator of STAT3 (Croker et al., 2003, 2012; Lang et al., 2003). Our data show that LPS stimulation resulted in higher transcription and protein levels of SOCS3 (Figure 2A–C), suggesting a role of this protein at the intersection between TLR4 and IL-6RA signaling. Moreover, pY-STAT3 levels were clearly reduced by culturing in the presence of MG132, a proteasome inhibitor that prevents degradation of SOCS3 (Figure 2D and E).

We then investigated cross-talk in the reverse direction, thus whether STAT3 activation would inhibit TLR responses, because IL-6 is known to inhibit dendritic cell maturation via STAT3 (Schindler et al., 1990; Park et al., 2004; Yu et al., 2007). Since TLR signaling promotes IL-6 synthesis (Supplementary Figure S2C), autocrine activation of STAT3 by IL-6 might lead to a negative feedback loop limiting cellular IL-6 production. To address this possibility, we performed siRNA gene silencing of IL-6RA (siIL-6RA) in moDCs and used non-targeting siRNA as a negative control (siCntrl). The levels of IL-6RA knockdown were sufficient (>95% by western blot, flow cytometry, and immunofluorescence microscopy) (Figure 2F; Supplementary Figure S3A and B) to attain ~80% blockage of IL-6 induced pY-STAT3 signaling (Figure 2G and H). Culturing IL-6RA-silenced moDCs in the presence of LPS for 4 h (i.e. the time after which we observed pY-STAT3 signaling; Figure 1D) increased both IL-6 transcription (by qPCR) and protein production (by ELISA) by ~2–3 folds compared to siCntrl (Figure 2I and J). These differences in IL-6 transcription and secretion disappeared after prolonged culturing with LPS (8 h) (Figure 2J and Supplementary Figure S3C), likely because of the refractory phase in which pY-STAT3 signaling is disabled by increased cellular levels of SOCS3 (Figure 2). Thus, LPS inhibits IL-6-induced pY-STAT3 signaling, whereas IL-6 reduces LPS-induced IL-6 production, suggesting that there is a mutual cross-inhibition between the IL-6 and the LPS signaling pathways in dendritic cells.

IL-6 signals from intracellular compartments

In hepatocytes, IL-6 predominantly signals from intracellular compartments of endosomal nature (Shah et al., 2006; Xu et al., 2007; German et al., 2011; Schmidt-Arras et al., 2014). We determined the subcellular localization of IL-6RA signaling in dendritic cells. First, we measured the fraction of IL-6RA present at the cell membrane and at intracellular organelles. MoDCs were immunostained with a monoclonal antibody recognizing the extracellular domain of IL-6RA both under permeabilizing and non-permeabilizing conditions and analyzed these stainings by flow cytometry. About 35% of IL-6RA was present at the plasma membrane, similar to the transferrin receptor (TfR) which also cycles via recycling endosomes to the plasma membrane (Figure 3A and Supplementary Figure S4A). Transmission electron microscopy experiments with immuno-gold antibody-conjugate uptake confirmed the presence of IL-6RA at intracellular compartments (Figure 3B and Supplementary Figure S4B). We performed immunofluorescence microscopy experiments to characterize the type of intracellular compartments where IL-6RA was residing. Because the signal of our IL-6RA antibody was too weak to resolve intracellular compartments (Supplementary Figure S3B), we visualized IL-6RA by overexpression of a construct coding for IL-6RA C-terminally fused to the fluorescent reporter protein mCherry. Fusion constructs of IL-6RA C-terminally conjugated to fluorescent proteins have been used previously to study IL-6RA trafficking and shedding (Chalaris et al., 2010). By immunofluorescence labeling, we observed localization of IL-6RA-mCherry at the plasma membrane and at an intracellular pool that overlapped with compartments positive for the early/recycling endosomal SNARE protein VAMP3, the early/late endosomal SNARE protein VAMP8 (Antonin et al., 2000), the trans-Golgi marker TGN38 (Murray et al., 2005), the recycling endosomal marker TfR, and less with the late endosomal/lysosomal marker LAMP1 and the early endosomal marker EEA1 (Figure 3C and D). These results indicate that IL-6RA traffics to the plasma membrane, the Golgi apparatus, recycling endosomes, and late endosomes/lysosomes.

Since our data show that the majority of IL-6RA locates at intracellular compartments in dendritic cells, and since IL-6RA

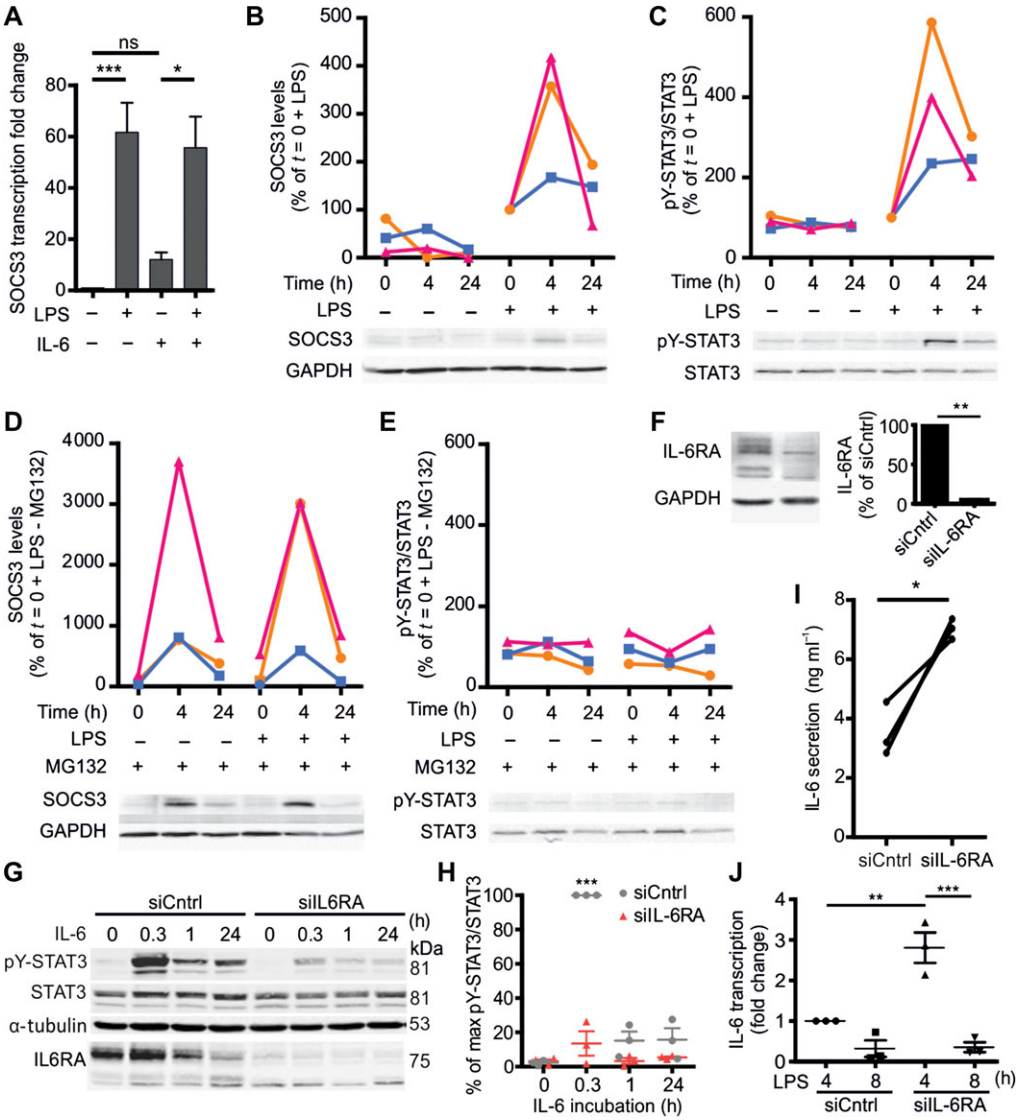

Figure 2 Cross-inhibition of IL-6 and LPS signaling in dendritic cells. (**A**) Quantification of SOCS3 mRNA levels in moDCs upon 4 h incubation in the presence or absence of LPS and/or IL-6. (**B** and **C**) moDCs were exposed to 0, 4, or 24 h LPS stimulation. The 0 h exposure to LPS was a quick wash in LPS-containing culture medium (<10 sec). SOCS3 protein levels (**B**) and tyrosine phosphorylated (Tyr705) pY-STAT3 over total STAT3 levels (**C**) were examined by western blot and quantified. For each donor, the relative levels were normalized to that of 0 h exposure to LPS stimulation. Representative blots (from the same donor) are shown and data from individual donors are shown in the graph. (**D** and **E**) moDCs were exposed to 0, 4, or 24 h LPS stimulation in the presence of the proteasome inhibitor MG132. SOCS3 levels (**D**) and pY-STAT3/STAT3 levels (**E**) were examined by western blot and then quantified. For each donor, the relative levels were normalized to that of 0 h LPS stimulation from **B**. Representative blots (from the same donor as shown in **B** and **C**) are shown and data from individual donors are shown in the graph. (**F**) Western blot showing IL-6RA levels in moDCs upon siRNA silencing of IL-6RA (siIL-6RA) and non-targeting siRNA (siCntrl). Bar graph: quantification (error bars represent SEM for six donors). (**G**) pY-STAT3 and IL-6RA levels in moDCs upon siIL-6RA and siCntrl treatment in the absence or presence of exogenous IL-6 for the indicated times. (**H**) Quantification of pY-STAT3/STAT3 in **G**. Data shown were from individual donors, normalized to the maximum pY-STAT3/STAT3 ratio for each donor. (**I**) IL-6 secretion by 4 h LPS-stimulated moDCs with or without siIL-6RA by ELISA (data from individual donors are shown). (**J**) IL-6 mRNA transcription in moDCs with or without siIL-6RA upon 4 or 8 h LPS incubation by qPCR.

signaling in hepatocytes is known to occur from intracellular compartments (Shah et al., 2006; Xu et al., 2007; German et al., 2011), we then tested for intracellular signaling of IL-6RA. Quantitative immunofluorescence experiments showed that exogenous IL-6 was taken up by the cells in a concentration-dependent manner (Figure 4A), with a similar concentration dependency as pY-STAT3 activation (Figure 1C). Although IL-6 exposure resulted in lower cellular levels of IL-6RA (Figures 2G

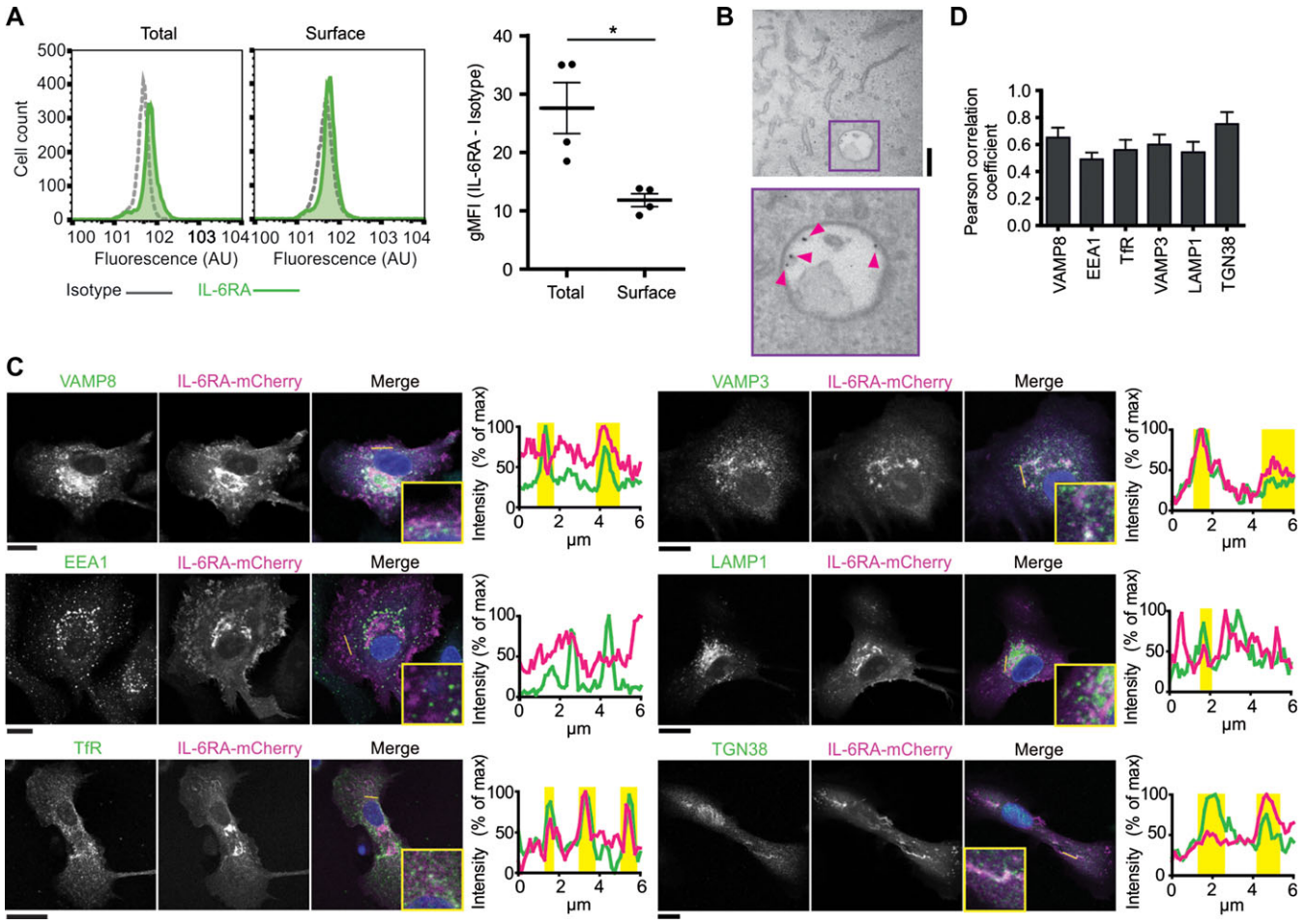

Figure 3 IL-6RA localizes at the plasma membrane, Golgi, and endosomes in dendritic cells. (**A**) Flow cytometry of moDCs immunostained for IL-6RA with (total) or without (surface) permeabilization. Geometric mean fluorescence intensities (gMFI) for individual donors are shown (isotype subtracted). (**B**) Transmission electron microscopy image of endocytosed antibody against IL-6RA labeled with Protein A-gold nanoparticles. Pink arrowheads indicate gold nanoparticles. Scale bar, 200 nm. (**C** and **D**) Confocal images (**C**) and quantification by Pearson correlation coefficients (**D**) of moDCs expressing IL-6RA fused to mCherry (magenta in merge; IL-6RA-mCherry) and immunolabeled for VAMP8, VAMP3, EEA1, LAMP1, TfR, or TGN38 (green). DAPI is in blue in merge. Graphs: fluorescence cross-sections as indicated. Yellow regions: overlap of IL-6RA-mCherry with organellar markers. Representative cells from multiple donors are shown (>7 cells/donor). Scale bar, 20 µm.

and 4B), as reported previously (Meley et al., 2017), we could not detect significant breakdown of exogenous IL-6 by the dendritic cells by quantitative ELISA (Supplementary Figure S5A–C). Although this apparent absence of IL-6 degradation might be caused by a too low sensitivity of the used assay, it at least shows that under our experimental conditions cellular breakdown did not have a measurable impact on extracellular IL-6 concentrations. IL-6 uptake by dendritic cells is important for signaling, because IL-6-dependent activation of pY-STAT3 could be almost completely blocked with the dynamin inhibitor hydroxy-dynasore (Figure 4C and Supplementary Figure S5D). Hydroxy-dynasore treatment increased IL-6RA localization at the plasma membrane by ~50% (Figure 4D), indicating that IL-6RA cycles via the plasma membrane to intracellular compartments. These findings support the signaling of IL-6 from intracellular compartments in dendritic cells, in a similar way as in hepatocytes, where IL-6 and IL-6RA are endocytosed in a dynamin-dependent manner and inhibition of dynamin results in impaired pY-STAT3 activation (Dittrich et al., 1994; Thiel et al., 1998; Shah et al., 2006; Xu et al., 2007; Schmidt-Arras et al., 2014).

The endosomal signaling of IL-6RA was further supported by live cell fluorescence microscopy experiments of dendritic cells expressing STAT3 fused to GFP (STAT3-GFP) which is retained at the nucleus upon activation (Shah et al., 2006; Ng et al., 2014). STAT3-GFP was co-expressed with a mCherry-tagged variant of the endocytic cargo adaptor Epsin 2 (Epsin2-mCherry) (Taylor et al., 2011). Overexpression of Epsin 2 acts as a dominant negative and blocks clathrin-mediated endocytosis by misguiding epidermal growth factor receptor substrate 15 and adapter protein 2 to overexpression foci (Rosenthal et al., 1999). Supporting a role for endocytosis in IL-6 signaling, the IL-6-induced translocation of STAT3-GFP to the nucleus was ~2-fold reduced in

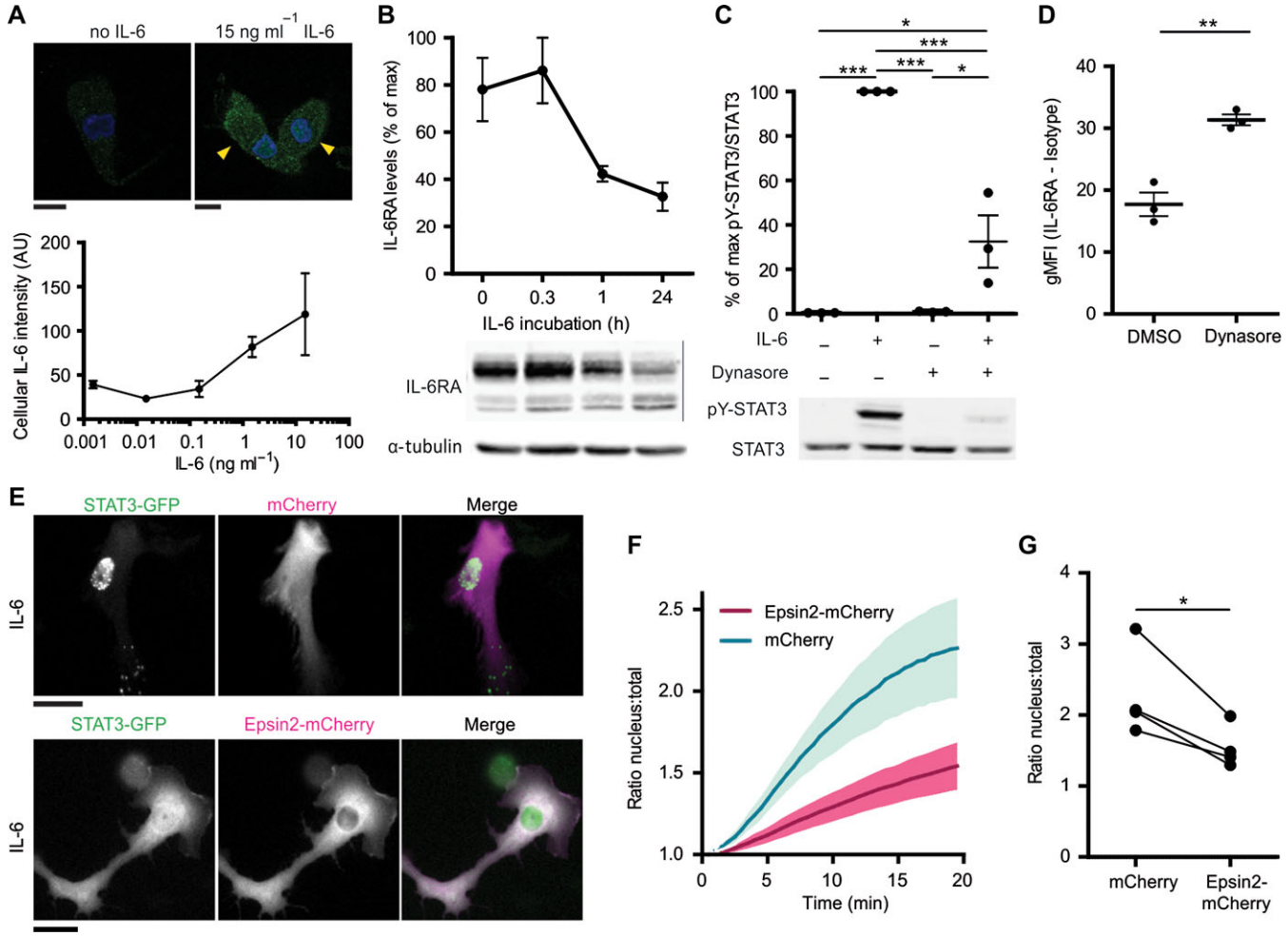

Figure 4 Endocytosis of IL-6 is required for paracrine STAT3 signaling. (**A**) MoDCs incubated with increasing concentrations of IL-6 for 20 min and immunostained for intracellular IL-6 (green) were imaged by confocal microscopy. DAPI is in blue. Yellow arrowheads indicate IL-6-positive cells. Graph: quantification of IL-6 signals (mean ± SEM from three donors). Scale bar, 10 μm. (**B**) Quantification of IL-6RA upon incubation with IL-6 for the indicated times by western blot (see also Figure 2G). Data were normalized to the highest IL-6RA band intensity per donor. α-tubulin is loading control. (**C**) STAT3 tyrosine 705 phosphorylation (pY-STAT3) of moDCs incubated with or without hydroxy-dynasore and/or 15 ng/ml IL-6. Graph: quantification for three different donors (mean ± SEM). Data were normalized to the highest pY-STAT3/STAT3 ratio per donor. (**D**) Flow cytometry of moDCs incubated with or without hydroxy-dynasore and immunostained for surface IL-6RA. gMFI of different donors are shown (isotype subtracted). (**E**) Fluorescence microscopy images of moDCs transfected with STAT3-GFP (green in merge) and only mCherry or Epsin2-mCherry (magenta in merge) and stimulated with IL-6 for 20 min. Scale bar, 20 μm (see also Supplementary Movies S1 and S2). (**F**) Quantification of STAT3-GFP retention at the nucleus following IL-6 stimulation in **E** (mean ± SEM for 80 cells from four donors). (**G**) Quantification of STAT3-GFP retention at the nucleus at 20 min after IL-6 stimulation for only mCherry (cntrl) or Epsin2-mCherry (from **F**; individual donor averages shown for 20–23 cells/donor).

dendritic cells expressing Epsin 2-mCherry compared to the control of mCherry alone (Figure 4E–G; Supplementary Movies S1 and S2). In some cells, we observed punctuated signals of STAT3-GFP in the cytosolic region (i.e. control condition of mCherry in Figure 4E), which might be caused by local STAT3 activation at endosomes, as reported in Hep3B cells (Xu et al., 2007). These results show that IL-6RA signals from intracellular compartments, and we next addressed whether *de novo* synthesized IL-6 in transit to the plasma membrane could also signal from these sites.

Intracellular signaling of newly synthesized IL-6 prior to secretion

In macrophages and dendritic cells, newly synthesized IL-6 does not traffic directly from the Golgi apparatus to the plasma membrane, but is instead routed via recycling endosomes that partially overlap with TfR and VAMP3 (Manderson et al., 2007; Verboogen et al., 2018). We performed fluorescence microscopy experiments to characterize the organelles of IL-6 trafficking. However, we only observed a very low signal of IL-6 in LPS-stimulated moDCs by immunofluorescence microscopy and flow

cytometry, and this signal was only observable at 4 h after LPS stimulation (Supplementary Figure S6A–C). As a positive control, inhibition of ER-Golgi trafficking with Brefeldin A (Bueno et al., 2001; Manderson et al., 2007) resulted in accumulation of IL-6 within the cells (Supplementary Figure S6A–C). SiRNA silencing of IL-6RA in moDCs, which blocks pY-STAT3 activation and results in higher IL-6 production (Figure 2F–J; Supplementary Figure S6E), also increased the intracellular accumulation of endogenous IL-6 compared to siCntrl by immunofluorescence microscopy and flow cytometry (Figure 5A and B). These results indicate that newly synthesized IL-6 does not accumulate within the majority of moDCs but is mostly secreted from these cells, as we reported previously (Verboogen et al., 2018) and has also been described for peripheral blood mononuclear cells (Schindler et al., 1990). In order to resolve the organelles involved in IL-6 trafficking, we increased the intracellular presence of IL-6 by overexpression of a construct coding for human IL-6 fused to GFP (IL-6-GFP). This strategy of overexpression of GFP-tagged IL-6 has been used previously to visualize intracellular trafficking of IL-6 (Manderson et al., 2007; Verboogen et al., 2018). We stimulated IL-6-GFP-transfected moDCs for 4 h with LPS and subsequently determined the subcellular localization of IL-6-GFP by immunofluorescence labeling with the same panel of organellar markers as we used previously for IL-6-RA (Figure 3C). Partial overlap of the IL-6-GFP signal was observed with the Golgi marker TGN38, the early/recycling endosomal markers EEA1 and VAMP3, the

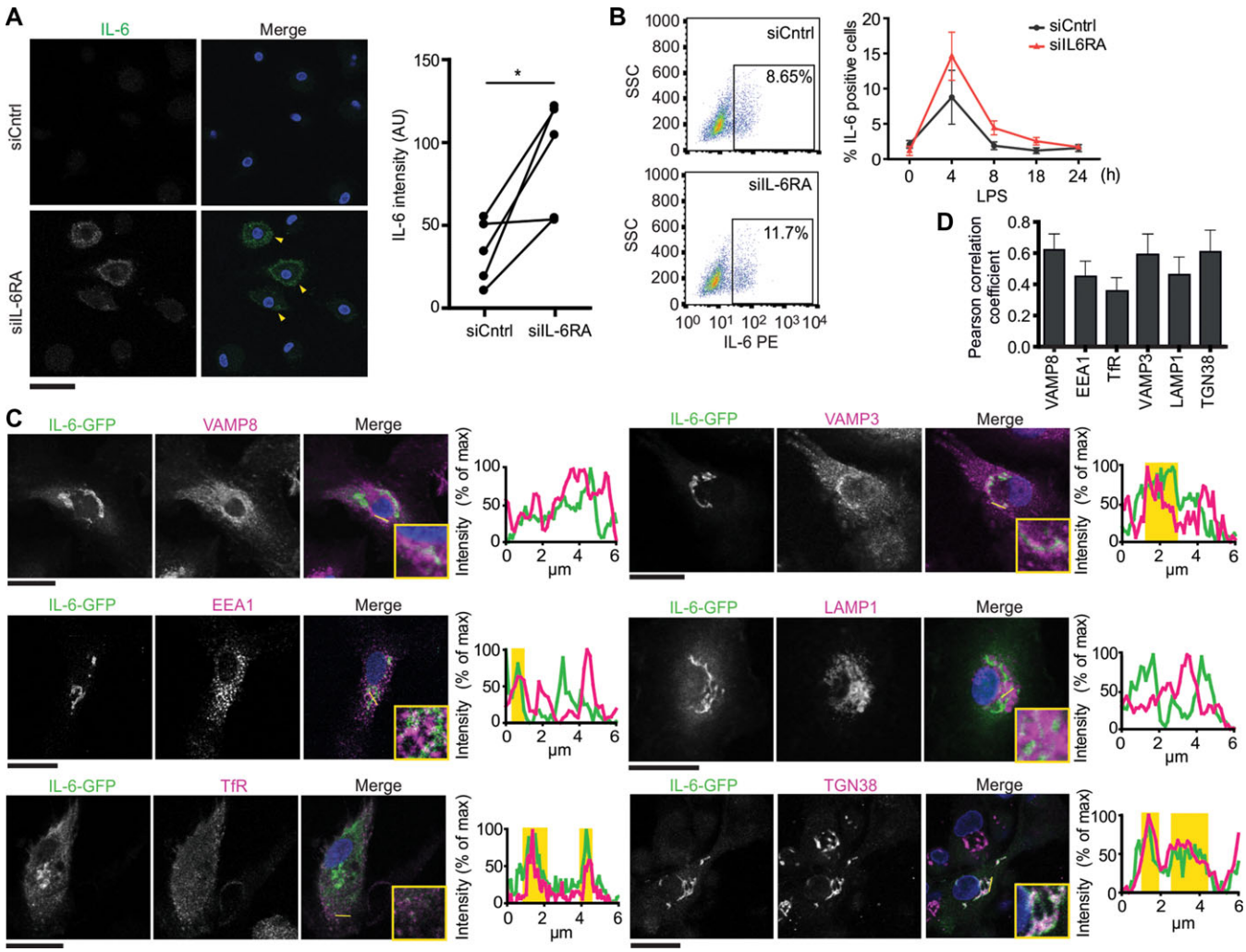

Figure 5 IL-6 is secreted via the Golgi apparatus and endosomes in dendritic cells. (**A**) Confocal micrographs of moDCs with siIL-6RA or control siRNA (siCntrl) and immunostained for IL-6 (green in merge). DAPI is in blue in merge. Yellow arrowheads indicate IL-6-positive cells. Graph: quantification of IL-6 fluorescence for individual donors. Scale bar, 50 μm. (**B**) Flow cytometry analysis of intracellular IL-6 accumulation in moDCs after siCntrl or siIL-6RA incubated with LPS for the indicated times (four individual donors; mean ± SEM; normalized to Brefeldin A-treated samples, see Supplementary Figure S6D). (**C** and **D**) Confocal images (**C**) and quantification by Pearson correlation coefficients (**D**) of moDCs expressing IL-6 fused to GFP (green in merge; IL-6-GFP) and immunolabeled for VAMP8, VAMP3, EEA1, LAMP1, TfR, or TGN38 (magenta). DAPI is in blue in merge. Graphs: fluorescence cross-sections as indicated. Yellow regions: overlap of IL-6-GFP and organellar markers. Representative cells from multiple donors are shown (>7 cells/donor). Scale bar, 20 μm.

late endosomal/lysosomal markers VAMP8 and LAMP1, and the TfR (Figure 5C and D). These results confirm that IL-6-GFP is secreted via the Golgi network and early/recycling endosomes, as previously reported for macrophages and dendritic cells (Manderson et al., 2007; Verboogen et al., 2018).

We then determined whether IL-6 would traffic via the same intracellular compartments as IL-6RA. Clear overlap of the IL-6-GFP and IL-6RA-mCherry signals was observed in moDCs co-transfected with both proteins, both in the absence and presence of LPS (Figure 6A), and as reported previously for BMDCs (Heink et al., 2017). Live cell time-lapse total-internal reflection fluorescence (TIRF) microscopy experiments confirmed that IL-6-GFP and IL-6RA-mCherry co-migrated to the plasma membrane (Figure 6B and Supplementary Movie S3). These experiments suggest that newly synthesized IL-6 in transit to the plasma membrane could encounter IL-6RA in intracellular compartments, which would enable auto-activation of STAT3. We performed flow chamber experiments to determine whether newly synthesized IL-6, and possibly other STAT3 activating factors such as IL-10 (Melillo et al., 2010), in transit to the plasma membrane would suffice for activation of STAT3. We kept moDCs under a constant flow, thereby continuously refreshing the LPS-supplemented medium and flushing away all secreted cytokines (Figure 6C). Under our experimental conditions, the concentration of IL-6 in the flow chamber remained well below 0.05 ng/ml which is far too low for STAT3 activation in the absence of LPS (Figures 1B, C and 6C). Nevertheless, LPS-induced pY-STAT3 activation could be detected under flow (Figure 6D), supporting the existence of self-signaling of newly synthesized IL-6 (and other factors) from intracellular compartments within the cells. To confirm this self-signaling of

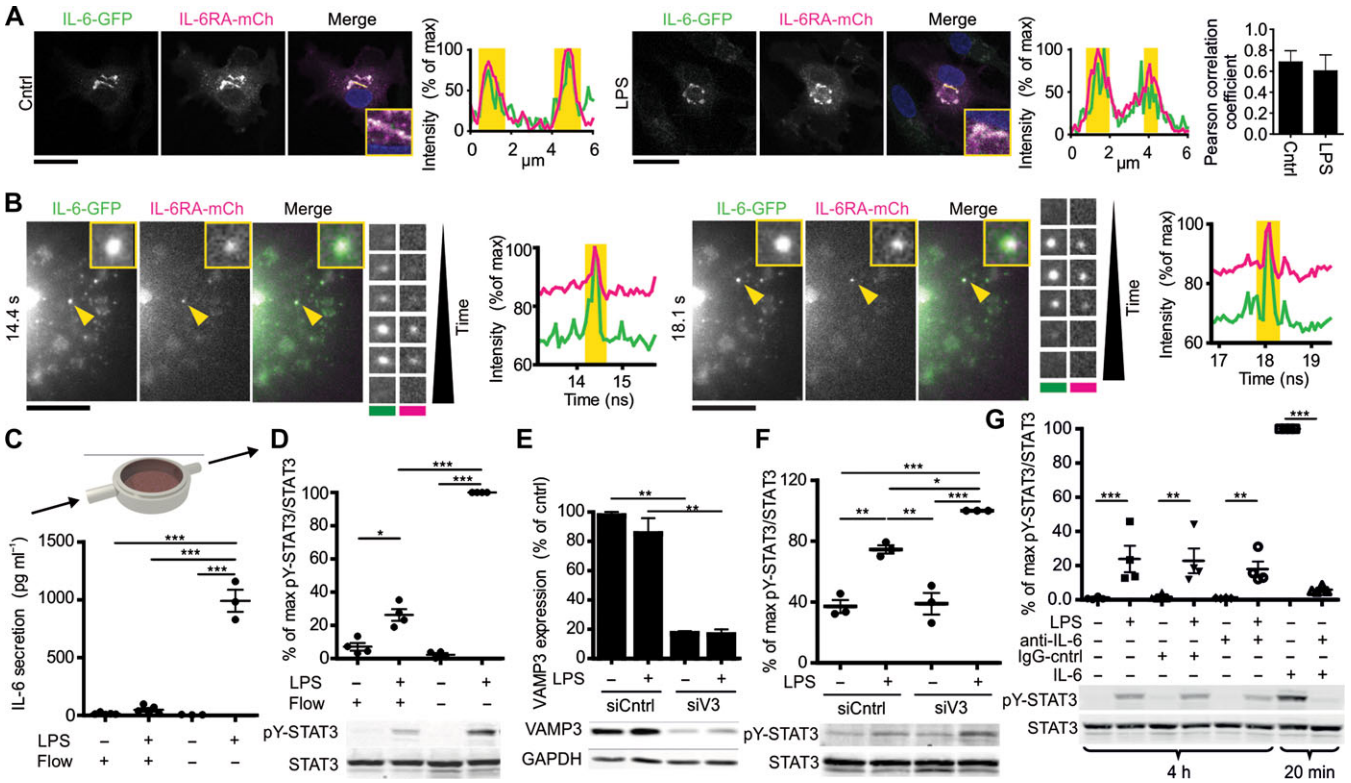

Figure 6 Signaling of newly synthesized IL-6 in transit to the plasma membrane. (**A**) Confocal images of moDCs co-expressing IL-6 fused to GFP (green in merge; IL-6-GFP) and IL-6RA fused to mCherry (magenta; IL-6RA-mCh) stimulated without or with LPS for 4 h. DAPI is in blue in merge. Graphs: fluorescence cross-sections as indicated. Yellow regions: overlap of IL-6-GFP and IL-6RA-mCherry. Bar graph: quantification of overlap by Pearson correlation coefficient (four donors; >7 cells/donor). Scale bar, 20 μm. (**B**) Stills from time-lapse TIRF microscopy of moDC overexpressing IL-6-GFP (green in merge) and IL-6RA-mCherry (magenta). Details of two exocytosis events indicated by the yellow arrowheads are shown. Graphs: quantification of the signals over time. Scale bar, 10 μm. Yellow regions: occurrence of exocytosis events (see also Supplementary Movie S3). (**C**) Scheme of the experimental setup for STAT3 activation under constant medium flow with or without LPS for 4 h. The graph shows the IL-6 concentrations in the supernatant from moDCs cultured in the presence or absence of LPS and with or without flow by ELISA. (**D**) Quantification of pY-STAT3 activation from moDCs in **C** for individual donors (mean ± SEM). Data were normalized to the highest pY-STAT3/STAT3 ratio per donor. (**E**) Quantification of VAMP3 after siRNA gene silencing (siV3) or non-targeting siRNA control (siCntrl) with or without 4 h LPS stimulation (mean ± SEM from 3 donors). GAPDH: loading control. (**F**) Quantification by western blot of pY-STAT3 activation after siV3 incubated with or without LPS for 4 h (mean ± SEM from 3 donors). (**G**) Quantification of pY-STAT3 activation upon incubation with 1 μg/ml LPS for 4 h or 15 ng/ml IL-6 for 20 min, in the absence or presence of an IL-6-neutralizing antibody (anti-IL-6) or IgG control (IgG-cntrl) (mean ± SEM from three donors). Representative western blots are shown.

newly synthesized IL-6, we performed siRNA knockdown of the SNARE protein VAMP3. VAMP3 mediates secretion of IL-6 and its knockdown results in impaired IL-6 secretion (Manderson et al., 2007; Boddul et al., 2014; Verboogen et al., 2017). VAMP3 knockdown also results in increased LPS-induced pY-STAT3 levels (Figure 6E and F), in line with intracellular self-signaling of newly synthesized IL-6. Finally, we performed experiments with an IL-6 neutralizing antibody that blocks IL-6 binding to the receptor (Figure 6G). Whereas this antibody could completely block pY-STAT3 activation triggered by extracellular IL-6, LPS-induced pY-STAT3 phosphorylation was not affected compared to conditions without antibody or isotype control (Figure 6G). Together, these findings support a model where newly synthesized IL-6 activates pY-STAT3 in transit to the plasma membrane from intracellular compartments.

Discussion

Endosomal signaling is emerging as an important principle for many different receptors, including receptor tyrosine kinases, insulin G protein-coupled receptors, and TLRs (Murphy et al., 2009; Platta and Stenmark, 2011). In this study, we show that although IL-6RA appears at the plasma membrane, IL-6-mediated tyrosine phosphorylation of STAT3 mainly occurs from intracellular compartments. This is in line with the finding that IL-6 and IL-6RA co-localize in intracellular compartments of BMDCs (Heink et al., 2017). In the hepatocyte cell lines HepG2 and HepB3, endosomal signaling of IL-6 (Shah et al., 2006; Xu et al., 2007; German et al., 2011; Schmidt-Arras et al., 2014) is proposed to promote STAT3-induced transcription by reducing the distance that STAT3 has to travel to the nucleus (German et al., 2011). A second potential role of endosomal signaling is that it might increase control over signaling, as receptors can be readily sorted to the lysosome for degradation or back to the plasma membrane for re-sensitization for the corresponding stimulus (Platta and Stenmark, 2011). In hepatocytes, IL-6 bound to IL-6RA and gp130 is internalized via the constitutive internalization of gp130 (Dittrich et al., 1994; Thiel et al., 1998) and the IL-6 receptor complex is subsequently degraded leading to a downregulation of the IL-6 receptor (Zohlnhöfer et al., 1992; Wang and Fuller, 1994; Heinrich et al., 1998; Blanchard et al., 2001). Also in dendritic cells, our data show that cellular levels of IL-6RA are reduced upon IL-6 stimulation, in line with previous findings (Meley et al., 2017), although we did not find evidence that breakdown of IL-6 itself resulted in a measurable reduction of extracellular IL-6 levels at our experimental conditions. Less efficient IL-6 degradation in dendritic cells compared with hepatocytes might well be physiological, since dendritic cells are major producers of IL-6 (Daudelin et al., 2013; Heink et al., 2017; Verboogen et al., 2017), whereas the liver is the major organ for removing IL-6 from circulation (Castell et al., 1990; Sonne et al., 1990).

A third potential role of intracellular interactions between IL-6 and IL-6RA is that it might facilitate organellar trafficking of IL-6. Our data indicate that these interactions already might occur within the Golgi and recycling endosomes. In macrophages, immuno-gold labeled IL-6 appeared consistently in close proximity to the luminal face of the membrane of recycling endosomes (Manderson et al., 2007), suggesting membrane association possibly by interactions with IL-6RA. IL-6RA thereby might act as an adapter molecule ensuring proper sorting of IL-6 to the correct target organelles. Such a mechanism would be reminiscent of the trafficking of newly formed IL-4 by the IL-4 receptor in eosinophils (Spencer et al., 2006). The trafficking of IL-6 by IL-6RA could explain how IL-6 can traverse through sub-compartments of recycling endosomes (Murray and Stow, 2014). This compartmentalization of recycling endosomes is the key to their sorting function, as it allows to direct cargo molecules in different directions, e.g. to the plasma membrane, to the Golgi apparatus, or to late endosomes/lysosomes (Wall et al., 2015). The trafficking of IL-6 by IL-6RA could also explain how IL-6 can be readily secreted after synthesis, with secretory vesicles containing only a limited number of IL-6 molecules and the majority of IL-6 producing cells showing no detectable intracellular pool of IL-6 (Verboogen et al., 2018).

A fourth potential role of co-trafficking of a complex of IL-6 with IL-6RA to the plasma membrane is that it may facilitate *trans*-signaling. *Trans*-signaling is the process by which a complex of (soluble) IL-6RA with IL-6 enables signaling of cells that do not express IL-6RA (but only gp130) (Taga et al., 1989) and largely underlies the proinflammatory role of IL-6 (Hunter and Jones, 2015; Schaper and Rose-John, 2015). *Trans*-presentation of IL-6 with IL-6RA on the surface of dendritic cells is responsible for the differentiation of pathogenic Th17 cells (Heink et al., 2017). Soluble gp130 counteracts this *trans*-signaling, as it sequesters the IL-6/IL-6RA complex and prevents it binding to full-length gp130 (Hunter and Jones, 2015; Schaper and Rose-John, 2015). IL-6RA in complex with IL-6 can also be cleaved from the membrane (Müllberg et al., 1993, 1994) by the metalloproteases ADAM10 and ADAM17 (Matthews et al., 2003; Yan et al., 2016; Zunke and Rose-John, 2017). As the K_{off} rate of IL-6 for IL-6RA is relatively low (Weiergräber et al., 1995), IL-6 will remain bound to IL-6RA for seconds to minutes after cleavage and this signaling complex could effectively potentiate cells in the vicinity. Such a release mechanism would be comparable with the signaling demonstrated for tumor necrosis factor α (TNFα), IL-15, and IL-11 (Schmid et al., 1995; Bulfone-Paus et al., 2006; Mortier et al., 2008; Lokau et al., 2016). For TNFα, ADAM17 cleaves its precursor at the plasma membrane resulting in release of TNFα (Black et al., 1997; Murray and Stow, 2014). The IL-11 receptor (IL-11R) is cleaved by ADAM10, making all gp130-positive cells sensitive to IL-11 induced STAT signaling, similar to soluble IL-6RA together with IL-6 (Taga et al., 1989; Lokau et al., 2016). IL-15 is cleaved at the plasma membrane together with IL-15 receptor subunit alpha (IL-15RA) (Bergamaschi et al., 2008; Duitman et al., 2008, 2011). However, in contrast to IL-6 with IL-6RA, IL-15RA is believed to remain associated with IL-15 and free IL-15 without IL-15RA does not, or only little, exist in circulation (Duitman et al., 2008, 2011; Bergamaschi et al., 2012).

Based on our data, we propose a fifth role of the intracellular signaling of IL-6. Our data show that self-activation of pY-STAT3

by newly synthesized IL-6 (and probably by other factors such as IL-10 (Melillo et al., 2010)) in transit to the plasma membrane results in a transient auto-inhibition of further IL-6 transcription (Figure 7). This negative feedback inhibition is caused by an antagonistic cross-talk between the LPS–TLR4–p38MAPK and IL-6–STAT3 pathways (Bode et al., 2012; Meley et al., 2017) and results in a short-term limit of IL-6 production by the dendritic cells. Our data show that during sustained exposure to LPS, this brake in IL-6 production is effectively shut off via the increased transcription and higher protein presence of SOCS3, which inhibits pY-STAT3 activity (Croker et al., 2003, 2012; Lang et al., 2003). This transient auto-inhibition of IL-6 synthesis by IL-6 signaling supports a new cellular mechanism by which the immune system might limit production of excessive IL-6 during sepsis or the invasion of microbial pathogens into the bloodstream. Following sepsis, an excessive systemic proinflammatory response can lead to tissue damage and organ failure and this so-called septic shock is a main cause of death in intensive care units (Schulte et al., 2013). IL-6 is a key mediator of septic shock as low serum levels of IL-6 are associated with a better prognosis and IL-6 levels in patients with septic shock are higher than in patients without shock (Hack et al., 1989; Damas et al., 1992; Spittler et al., 2000; Chaudhry et al., 2013). *In vivo* studies in IL-6-knockout mice demonstrated that LPS administration leads to higher levels of proinflammatory cytokines such as TNFα (Xing et al., 1998) and they do not develop the hypothermia characteristic of early sepsis and show less weight loss compared to wild-type mice (Remick et al., 2005). Moreover, the absence of the IL-6 gene in mouse models of acute infection decreases inflammatory responses and protects from mortality and organ failure (Cuzzocrea et al., 1999). In humans, IL-6 was identified as a key mediator of myocardial depression in septic shock, which leads to impaired tissue perfusion, multi-organ failure, and death (Pathan et al., 2004). Thus, excessive IL-6 secretion following acute infection can be detrimental (Tanaka et al., 2016), and the transient restraining of IL-6 production by self-signaling of newly produced IL-6 might be beneficial.

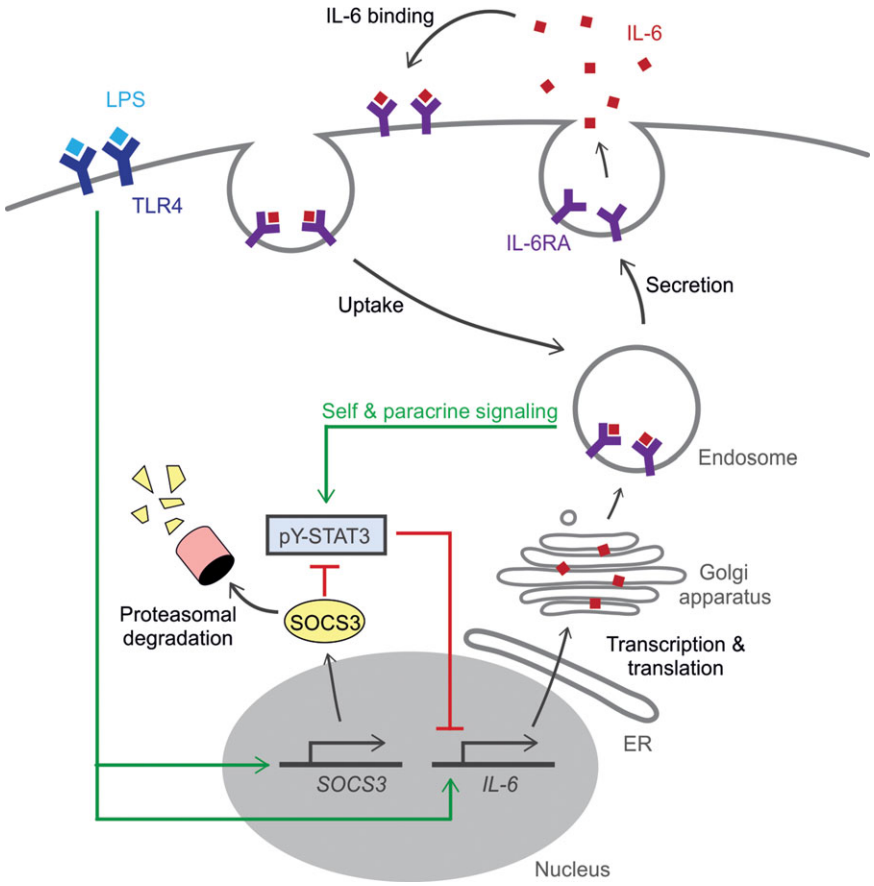

Figure 7 Self-signaling of IL-6RA at intracellular compartments limits IL-6 synthesis by dendritic cells. Model scheme depicting the interplay of synthesis, trafficking, and intracellular signaling of IL-6. LPS binding to TLR4 promotes the transcription of IL-6 and SOCS3. SOCS3 is rapidly degraded by the proteasome. Newly synthesized IL-6 in transit to the plasma membrane self-signals from endosomal compartments prior to secretion. Extracellular IL-6 is taken up by the cell and also signals from endosomal compartments. This leads to an increased pY-STAT3 activation (phosphorylation of Tyr705), which represses the transcription of IL-6. pY-STAT3 activation, in turn, is inhibited by the increased level of SOCS3. ER, endoplasmic reticulum.

Materials and methods

MoDCs were derived from peripheral blood monocytes from healthy volunteers (informed consent obtained and according to institutional and national ethics guidelines) by culturing with IL-4 and GM-CSF. Experimental details for the cell culture, PCR, transfection, western blot, microscopy, and statistical analysis are described in the Supplementary material.

Supplementary material

Supplementary material is available at *Journal of Molecular Cell Biology* online.

Acknowledgements

We thank Christien Merrifield for the Epsin2 construct.

Funding

This work was supported by a Starting Grant from the European Research Council (ERC) under the Seventh Framework Programme FP7-IDEAS-ERC (Grant Agreement Number 336479). G.v.d.B. is funded by the following grants: a Hypathia Tenure Track Research Fellowship from the Radboud University Medical Center, a Career Development Award from the Human Frontier Science Program, a Gravitation Programme 2013 Grant from the Netherlands Organization for Scientific Research (NWO, Nederlandse Organisatie voor Wetenschappelijk Onderzoek) (ICI-024.002.009), and a Vidi grant from the NWO Talent Scheme (NWO-ALW 864.14.001). N.H.R. is funded by a Long-Term Fellowship from the European Molecular Biology Organization (EMBO-LTF, ALTF 232-2016) and a Veni grant from the NWO Talent Scheme (016.Veni.171.097).

Conflict of interest: none declared.

References

Antonin, W., Holroyd, C., Tikkanen, R., et al. (2000). The R-SNARE endobrevin/VAMP-8 mediates homotypic fusion of early endosomes and late endosomes. Mol. Biol. Cell *11*, 3289–3298.

Bergamaschi, C., Bear, J., Rosati, M., et al. (2012). Circulating IL-15 exists as heterodimeric complex with soluble IL-15Rα in human and mouse serum. Blood *120*, e1–e8.

Bergamaschi, C., Rosati, M., Jalah, R., et al. (2008). Intracellular interaction of interleukin-15 with its receptor alpha during production leads to mutual stabilization and increased bioactivity. J. Biol. Chem. *283*, 4189–4199.

Bhattacharjee, A., Xu, B., Frank, D.A., et al. (2006). Monocyte 15-lipoxygenase expression is regulated by a novel cytosolic signaling complex with protein kinase C and tyrosine-phosphorylated Stat3. J. Immunol. *177*, 3771–3781.

Black, R.A., Rauch, C.T., Kozlosky, C.J., et al. (1997). A metalloproteinase disintegrin that releases tumour-necrosis factor-α from cells. Nature *385*, 729–733.

Blanchard, F., Wang, Y., Kinzie, E., et al. (2001). Oncostatin M regulates the synthesis and turnover of gp130, leukemia inhibitory factor receptor alpha, and oncostatin M receptor beta by distinct mechanisms. J. Biol. Chem. *276*, 47038–47045.

Boddul, S.V., Meng, J., Dolly, J.O., et al. (2014). SNAP-23 and VAMP-3 contribute to the release of IL-6 and TNFα from a human synovial sarcoma cell line. FEBS J. *281*, 750–765.

Bode, J.G., Ehlting, C., and Häussinger, D. (2012). The macrophage response towards LPS and its control through the p38(MAPK)-STAT3 axis. Cell. Signal. *24*, 1185–1194.

Bueno, C., Almeida, J., Alguero, M.C., et al. (2001). Flow cytometric analysis of cytokine production by normal human peripheral blood dendritic cells and monocytes: comparative analysis of different stimuli, secretion-blocking agents and incubation periods. Cytometry *46*, 33–40.

Bulfone-Paus, S., Bulanova, E., Budagian, V., et al. (2006). The interleukin-15/interleukin-15 receptor system as a model for juxtacrine and reverse signaling. Bioessays *28*, 362–377.

Castell, J., Klapproth, J., Gross, V., et al. (1990). Fate of interleukin-6 in the rat. Involvement of skin in its catabolism. Eur. J. Biochem. *189*, 113–118.

Chalaris, A., Gewiese, J., Paliga, K., et al. (2010). ADAM17-mediated shedding of the IL6R induces cleavage of the membrane stub by γ-secretase. Biochim. Biophys. Acta *1803*, 234–245.

Chaudhry, H., Zhou, J., Zhong, Y., et al. (2013). Role of cytokines as a double-edged sword in sepsis. In Vivo *27*, 669–684.

Croker, B.A., Kiu, H., Pellegrini, M., et al. (2012). IL-6 promotes acute and chronic inflammatory disease in the absence of SOCS3. Immunol. Cell Biol. *90*, 124–129.

Croker, B.A., Krebs, D.L., Zhang, J.-G., et al. (2003). SOCS3 negatively regulates IL-6 signaling in vivo. Nat. Immunol. *4*, 540–545.

Cuzzocrea, S., de Sarro, G., Costantino, G., et al. (1999). Role of interleukin-6 in a non-septic shock model induced by zymosan. Eur. Cytokine Netw. *10*, 191–203.

Damas, P., Ledoux, D., Nys, M., et al. (1992). Cytokine serum level during severe sepsis in human IL-6 as a marker of severity. Ann. Surg. *215*, 356–362.

Daudelin, J.-F., Mathieu, M., Boulet, S., et al. (2013). IL-6 production by dendritic cells is dispensable for $CD8^+$ memory T-cell generation. Biomed. Res. Int. *2013*, 126189.

Dittrich, E., Rose-John, S., Gerhartz, C., et al. (1994). Identification of a region within the cytoplasmic domain of the interleukin-6 (IL-6) signal transducer gp130 important for ligand-induced endocytosis of the IL-6 receptor. J. Biol. Chem. *269*, 19014–19020.

Duitman, E.H., Orinska, Z., Bulanova, E., et al. (2008). How a cytokine is chaperoned through the secretory pathway by complexing with its own receptor: lessons from interleukin-15 (IL-15)/IL-15 receptor alpha. Mol. Cell. Biol. *28*, 4851–4861.

Duitman, E.H., Orinska, Z., and Bulfone-Paus, S. (2011). Mechanisms of cytokine secretion: a portfolio of distinct pathways allows flexibility in cytokine activity. Eur. J. Cell Biol. *90*, 476–483.

Ernst, M., and Jenkins, B.J. (2004). Acquiring signalling specificity from the cytokine receptor gp130. Trends Genet. *20*, 23–32.

Galdiero, M., Vitiello, M., D'Isanto, M., et al. (2006). STAT1 and STAT3 phosphorylation by porins are independent of JAKs but are dependent on MAPK pathway and plays a role in U937 cells production of interleukin-6. Cytokine *36*, 218–228.

Garbers, C., Aparicio-Siegmund, S., and Rose-John, S. (2015). The IL-6/gp130/STAT3 signaling axis: recent advances towards specific inhibition. Curr. Opin. Immunol. *34*, 75–82.

German, C.L., Sauer, B.M., and Howe, C.L. (2011). The STAT3 beacon: IL-6 recurrently activates STAT 3 from endosomal structures. Exp. Cell Res. *317*, 1955–1969.

Grossman, R.M., Krueger, J., Yourish, D., et al. (1989). Interleukin 6 is expressed in high levels in psoriatic skin and stimulates proliferation of cultured human keratinocytes. Proc. Natl Acad. Sci. USA *86*, 6367–6371.

Hack, C.E., De Groot, E.R., Felt-Bersma, R.J.F., et al. (1989). Increased plasma levels of interleukin-6 in sepsis. Blood *74*, 1704–1710.

Hammacher, A., Ward, L.D., Weinstock, J., et al. (1994). Structure-function analysis of human IL-6: identification of two distinct regions that are important for receptor binding. Protein Sci. *3*, 2280–2293.

Heink, S., Yogev, N., Garbers, C., et al. (2017). Trans-presentation of IL-6 by dendritic cells is required for the priming of pathogenic TH17 cells. Nat. Immunol. *18*, 74–85.

Heinrich, P.C., Behrmann, I., Müller-Newen, G., et al. (1998). Interleukin-6-type cytokine signalling through the gp130/Jak/STAT pathway. Biochem. J. *334*, 297–314.

Helfgott, D.C., Tatter, S.B., Santhanam, U., et al. (1989). Multiple forms of IFN-β2/IL-6 in serum and body fluids during acute bacterial infection. J. Immunol. *142*, 948–953.

Horiuchi, S., Koyanagi, Y., Zhou, Y., et al. (1994). Soluble interleukin-6 receptors released from T cell or granulocyte/macrophage cell lines and human peripheral blood mononuclear cells are generated through an alternative splicing mechanism. Eur. J. Immunol. *24*, 1945–1948.

Hunter, C., and Jones, S. (2015). IL-6 as a keystone cytokine in health and disease. Nat. Immunol. *16*, 448–457.

Hwang, W., Jung, K., Jeon, Y., et al. (2010). Knockdown of the interleukin-6 receptor alpha chain of dendritic cell vaccines enhances the therapeutic potential against IL-6 producing tumors. Vaccine *29*, 34–44.

Jonuleit, H., Kühn, U., Müller, G., et al. (1997). Pro-inflammatory cytokines and prostaglandins induce maturation of potent immunostimulatory dendritic cells under fetal calf serum-free conditions. Eur. J. Immunol. *27*, 3135–3142.

Kimura, A., and Kishimoto, T. (2010). IL-6: regulator of Treg/Th17 balance. Eur. J. Immunol. *40*, 1830–1835.

Kumolosasi, E., Salim, E., Jantan, I., et al. (2014). Kinetics of intracellular, extracellular and production of pro-inflammatory cytokines in lipopolysaccharide-stimulated human peripheral blood mononuclear cells. Trop. J. Pharm. Res. *13*, 536.

Lang, R., Pauleau, A.-L., Parganas, E., et al. (2003). SOCS3 regulates the plasticity of gp130 signaling. Nat. Immunol. *4*, 546–550.

Larregina, A.T., Morelli, A.E., Kolkowski, E., et al. (1997). Pattern of cytokine receptors expressed by human dendritic cells migrated from dermal explants. Immunology *91*, 303–313.

Lokau, J., Nitz, R., Agthe, M., et al. (2016). Proteolytic cleavage governs interleukin-11 trans-signaling. Cell Rep. *14*, 1761–1773.

Luig, M., Kluger, M.A., Goerke, B., et al. (2015). Inflammation-Induced IL-6 functions as a natural brake on macrophages and limits GN. J. Am. Soc. Nephrol. *26*, 1597–1607.

Manderson, A.P., Kay, J.G., Hammond, L., et al. (2007). Subcompartments of the macrophage recycling endosome direct the differential secretion of IL-6 and TNFα. J. Cell Biol. *178*, 57–69.

Matthews, V., Schuster, B., Schütze, S., et al. (2003). Cellular cholesterol depletion triggers shedding of the human interleukin-6 receptor by ADAM10 and ADAM17 (TACE). J. Biol. Chem. *278*, 38829–28839.

May, L.T., Patel, K., García, D., et al. (1994). Sustained high levels of circulating chaperoned interleukin-6 after active specific cancer immunotherapy. Blood *84*, 1887–1895.

May, L.T., Viguet, H., Kenney, J.S., et al. (1992). High levels of 'complexed' interleukin-6 in human blood. J. Biol. Chem. *267*, 19698–19704.

McFarland-Mancini, M.M., Funk, H.M., Paluch, A.M., et al. (2010). Differences in wound healing in mice with deficiency of IL-6 versus IL-6 receptor. J. Immunol. *184*, 7219–7228.

Meley, D., Héraud, A., Gouilleux-Gruart, V., et al. (2017). Tocilizumab contributes to the inflammatory status of mature dendritic cells through interleukin-6 receptor subunits modulation. Front. Immunol. *8*, 926.

Melillo, J.A., Song, L., Bhagat, G., et al. (2010). Dendritic cell (DC)-specific targeting reveals Stat3 as a negative regulator of DC function. J. Immunol. *184*, 2638–2645.

Moravcová, S., Červená, K., Pačesová, D., et al. (2016). Identification of STAT3 and STAT5 proteins in the rat suprachiasmatic nucleus and the Day/Night difference in astrocytic STAT3 phosphorylation in response to lipopolysaccharide. J. Neurosci. Res. *94*, 99–108.

Mortier, E., Woo, T., Advincula, R., et al. (2008). IL-15Rα chaperones IL-15 to stable dendritic cell membrane complexes that activate NK cells via trans presentation. J. Exp. Med. *205*, 1213–1225.

Müllberg, J., Oberthür, W., Lottspeich, F., et al. (1994). The soluble human IL-6 receptor. Mutational characterization of the proteolytic cleavage site. J. Immunol. *152*, 4958–4968.

Müllberg, J., Schooltink, H., Stoyan, T., et al. (1993). The soluble interleukin-6 receptor is generated by shedding. Eur. J. Immunol. *23*, 473–480.

Murphy, J.E., Padilla, B.E., Hasdemir, B., et al. (2009). Endosomes: a legitimate platform for the signaling train. Proc. Natl Acad. Sci. USA *106*, 17615–17622.

Murray, R.Z., Kay, J.G., Sangermani, D.G., et al. (2005). A role for the phagosome in cytokine secretion. Science *310*, 1492–1495.

Murray, R.Z., and Stow, J.L. (2014). Cytokine secretion in macrophages: SNAREs, rabs, and membrane trafficking. Front. Immunol. *5*, 538.

Ndubuisi, M.I., Patel, K., Rayanade, R.J., et al. (1998). Distinct classes of chaperoned IL-6 in human blood: differential immunological and biological availability. J. Immunol. *160*, 494–501.

Ng, I.H.W., Bogoyevitch, M.A., and Jans, D.A. (2014). Cytokine-induced slowing of STAT3 nuclear import; faster basal trafficking of the STAT3β isoform. Traffic *15*, 946–960.

Niemand, C., Nimmesgern, A., Haan, S., et al. (2003). Activation of STAT3 by IL-6 and IL-10 in primary human macrophages is differentially modulated by suppressor of cytokine signaling 3. J. Immunol. *170*, 3263–3272.

Nowell, M.A., Richards, P.J., Horiuchi, S., et al. (2003). Soluble IL-6 receptor governs IL-6 activity in experimental arthritis: blockade of arthritis severity by soluble glycoprotein 130. J. Immunol. *171*, 3202–3209.

Park, S.-J., Nakagawa, T., Kitamura, H., et al. (2004). IL-6 regulates in vivo dendritic cell differentiation through STAT3 activation. J. Immunol. *173*, 3844–3854.

Pathan, N., Hemingway, C., Alizadeh, A., et al. (2004). Role of interleukin 6 in myocardial dysfunction of meningococcal septic shock. Lancet *363*, 203–209.

Platta, H.W., and Stenmark, H. (2011). Endocytosis and signaling. Curr. Opin. Cell Biol. *23*, 393–403.

Remick, D.G., Bolgos, G., Copeland, S., et al. (2005). Role of interleukin-6 in mortality from and physiologic response to sepsis. Infect. Immun. *73*, 2751–2757.

Robak, T., Gladalska, A., Stepien94, H., et al. (1998). Serum levels of interleukin-6 type cytokines and soluble interleukin-6 receptor in patients with rheumatoid arthritis. Mediators Inflamm. *7*, 347–353.

Rosenthal, J.A., Chen, H., Slepnev, V.I., et al. (1999). The epsins define a family of proteins that interact with components of the clathrin coat and contain a new protein module. J. Biol. Chem. *274*, 33959–33965.

Salgado, R., Junius, S., Benoy, I., et al. (2003). Circulating interleukin-6 predicts survival in patients with metastatic breast cancer. Int. J. Cancer *103*, 642–646.

Schaper, F., and Rose-John, S. (2015). Interleukin-6: Biology, signaling and strategies of blockade. Cytokine Growth Factor Rev. *26*, 475–487.

Schindler, R., Mancilla, J., Endres, S., et al. (1990). Correlations and interactions in the production of interleukin-6 (IL-6), IL-1, and tumor necrosis factor (TNF) in human blood mononuclear cells: IL-6 suppresses IL-1 and TNF. Blood *75*, 40–47.

Schmid, E.F., Binder, K., Grell, M., et al. (1995). Both tumor necrosis factor receptors, TNFR60 and TNFR80, are involved in signaling endothelial tissue factor expression by juxtacrine tumor necrosis factor α. Blood *86*, 1836–1841.

Schmidt-Arras, D., Müller, M., Stevanovic, M., et al. (2014). Oncogenic deletion mutants of gp130 signal from intracellular compartments. J. Cell Sci. *127*, 341–353.

Schulte, W., Bernhagen, J., and Bucala, R. (2013). Cytokines in sepsis: potent immunoregulators and potential therapeutic targets—an updated view. Mediators Inflamm. *2013*, 165974.

Shah, M., Patel, K., Mukhopadhyay, S., et al. (2006). Membrane-associated STAT3 and PY-STAT3 in the cytoplasm. J. Biol. Chem. *281*, 7302–7308.

Shimamoto, K., Ito, T., Ozaki, Y., et al. (2013). Serum interleukin 6 before and after therapy with tocilizumab is a principal biomarker in patients with rheumatoid arthritis. J. Rheumatol. *40*, 1074–1081.

Silver, J.S., and Hunter, C. (2010). gp130 at the nexus of inflammation, autoimmunity, and cancer. J. Leukoc. Biol. *88*, 1145–1156.

Sonne, O., Davidsen, O., Møller, B.K., et al. (1990). Cellular targets and receptors for interleukin-6. I. In vivo and in vitro uptake of IL-6 in liver and hepatocytes. Eur. J. Clin. Invest. *20*, 366–376.

Spencer, L.A., Melo, R.C.N., Perez, S.A.C., et al. (2006). Cytokine receptor-mediated trafficking of preformed IL-4 in eosinophils identifies an innate immune mechanism of cytokine secretion. Proc. Natl Acad. Sci. USA *103*, 3333–3338.

Spittler, A., Razenberger, M., Kupper, H., et al. (2000). Relationship between interleukin-6 plasma concentration in patients with sepsis, monocyte phenotype, monocyte phagocytic properties, and cytokine production. Clin. Infect. Dis. *31*, 1338–1342.

Taga, T., Hibi, M., Hirata, Y., et al. (1989). Interleukin-6 triggers the association of its receptor with a possible signal transducer, gp130. Cell *58*, 573–581.

Tanaka, T., Narazaki, M., and Kishimoto, T. (2016). Immunotherapeutic implications of IL-6 blockade for cytokine storm. Immunotherapy *8*, 959–970.

Taylor, M.J., Perrais, D., and Merrifield, C.J. (2011). A high precision survey of the molecular dynamics of mammalian clathrin-mediated endocytosis. PLoS Biol. *9*, e1000604.

Thiel, S., Dahmen, H., Martens, A., et al. (1998). Constitutive internalization and association with adaptor protein-2 of the interleukin-6 signal transducer gp130. FEBS Lett. *441*, 231–234.

van Bon, L., Popa, C., Huijbens, R., et al. (2010). Distinct evolution of TLR-mediated dendritic cell cytokine secretion in patients with limited and diffuse cutaneous systemic sclerosis. Ann. Rheum. Dis. *69*, 1539–1547.

Verboogen, D.R.J., González Mancha, N., Ter Beest, M., et al. (2017). Fluorescence lifetime imaging microscopy reveals rerouting of SNARE trafficking driving dendritic cell activation. Elife *6*, 1–17.

Verboogen, D.R.J., ter Beest, M., Honigmann, A., et al. (2018). Secretory vesicles of immune cells contain only a limited number of interleukin 6 molecules. FEBS Lett. *592*, 1535–1544.

Waage, A., Brandtzaeg, P., Halstensen, A., et al. (1989). The complex pattern of cytokines in serum from patients with meningococcal septic shock. Association between interleukin 6, interleukin 1, and fatal outcome. J. Exp. Med. *169*, 333–338.

Wall, A.A., Condon, N.D., Yeo, J.C., et al. (2015). Dynamic imaging of the recycling endosomal network in macrophages. Methods Cell Biol. *130*, 1–18.

Wang, Y., and Fuller, G.M. (1994). Phosphorylation and internalization of gp130 occur after IL-6 activation of Jak2 kinase in hepatocytes. Mol. Biol. Cell *5*, 819–828.

Wang, T., Niu, G., Kortylewski, M., et al. (2004). Regulation of the innate and adaptive immune responses by Stat-3 signaling in tumor cells. Nat. Med. *10*, 48–54.

Weiergräber, O., Hemmann, U., Küster, A., et al. (1995). Soluble human interleukin-6 receptor. Expression in insect cells, purification and characterization. Eur. J. Biochem. *234*, 661–669.

Wen, Z., Zhong, Z., and Darnell, J.E. (1995). Maximal activation of transcription by Stat1 and Stat3 requires both tyrosine and serine phosphorylation. Cell *82*, 241–250.

Wolf, J., Rose-John, S., and Garbers, C. (2014). Interleukin-6 and its receptors: a highly regulated and dynamic system. Cytokine *70*, 11–20.

Xing, Z., Gauldie, J., Cox, G., et al. (1998). IL-6 is an antiinflammatory cytokine required for controlling local or systemic acute inflammatory responses. J. Clin. Invest. *101*, 311–320.

Xu, F., Mukhopadhyay, S., and Sehgal, P.B. (2007). Live cell imaging of interleukin-6-induced targeting of 'transcription factor' STAT3 to sequestering endosomes in the cytoplasm. Am. J. Physiol. Cell Physiol. *293*, C1374–C1382.

Xu, J., Ye, Y., Zhang, H., et al. (2016). Diagnostic and prognostic value of serum interleukin-6 in colorectal cancer. Medicine *95*, e2502.

Yamasaki, K., Taga, T., Hirata, Y., et al. (1988). Cloning and expression of the human interleukin-6 (BSF-2/IFNβ2) receptor. Science *241*, 825–828.

Yan, I., Schwarz, J., Lücke, K., et al. (2016). ADAM17 controls IL-6 signaling by cleavage of the murine IL-6Rα from the cell surface of leukocytes during inflammatory responses. J. Leukoc. Biol. *99*, 749–760.

Yokogami, K., Wakisaka, S., Avruch, J., et al. (2000). Serine phosphorylation and maximal activation of STAT3 during CNTF signaling is mediated by the rapamycin target mTOR. Curr. Biol. *10*, 47–50.

Yu, H., Kortylewski, M., and Pardoll, D. (2007). Crosstalk between cancer and immune cells: role of STAT3 in the tumour microenvironment. Nat. Rev. Immunol. *7*, 41–51.

Zohlnhöfer, D., Graeve, L., Rose-John, S., et al. (1992). The hepatic interleukin-6 receptor. Down-regulation of the interleukin-6 binding subunit (gp80) by its ligand. FEBS Lett. *306*, 219–222.

Zunke, F. and Rose-John, S. (2017). The shedding protease ADAM17: physiology and pathophysiology. Biochim. Biophys. Acta *1864*, 2059–2070.